مجلة الدراسات التربوية والعلمية - كلية التربية - الجامعة العراقية
العدد الثاني والعشرون - المجلد الثاني - علوم الفيزياء - أيلول 2023 م
doi.org/10.52866/esj.2023.02.22.09

Modulating ZnO Thin Film Nanostructures via Cobalt-Doping by Spray Pyrolysis and their Effects on Optical and Structural Properties

Anas A. Abdullah
Iraq, Ministry of Education General Directorate of Education in Salah al-Din
anasabdabdullah@gmail.com

Abstract:

In this study, root-like nanostructures of ZnO were synthesized via the spray pyrolysis technique. The process involved depositing a metal acetate solution onto a heated platform maintained at 400 °C, with controlled deposition rates. Simultaneously, incremental incorporation of Cobalt dopants into the ZnO matrix led to gradual enlargement of the root branches' diameter. Structural insight was gained through X-ray diffraction (XRD) analysis, revealing successful Cobalt dopant integration up to x=0.2 with coherent solubility. However, higher Co/Zn atomic ratios, exceeding 0.2 , revealed the emergence of additional minor phase of cobalt oxide. Optical characteristics exhibited notable variations tied to Cobalt concentration. Optical absorbance increased proportionally with elevated Cobalt content, while conversely, energy bandgap reduced as Co content increased. These findings collectively highlight the controllable synthesis of root-like ZnO nanostructures via spray pyrolysis, modulated by Cobalt dopants.

Key words: Nanostructure engineering, Thin film metal oxide, Cobalt-doped ZnO .

تعديل الهياكل النانوية ذات الأغشية الرقيقة من أكسيد الزنك عن طريق التشويب بالكوبالت عن طريق الانحلال الحراري بالرش وتأثيراتها على الخصائص البصرية والتركيبية

أنس عبد عبد الله
العراق، وزارة التربية المديرية العامة لتربية صلاح الدين
anasabdabdallah@gmail.com

مستخلص:

تم في هذه الدراسة تشكيل هياكل نانوية تشبه الجذور من أكسيد الزنك عبر تقنية الانحلال الحراري بالرش. تضمنت العملية ترسيب محلول خلات معدنية على منصة ساخنة ثابتة الحرارة عند 400 درجة مئوية، مع التحكم في معدلات ترسيب. في الوقت نفسه، أدى الدمج المتزايد لشوائب الكوبالت في مصفوفة أكسيد الزنك إلى توسيع تدريجي لقطر فروع الجذر. تم الحصول على رؤية هيكلية من خلال تحليل حيود الأشعة السينية (XRD)، مما يكشف عن اندماج ناجح لمادة الكوبالت يصل إلى 0.2 = x مع قابلية ذوبان متماسكة. ومع ذلك، فإن ارتفاع النسب الذرية Co/Zn، التي تجاوزت 0.2، كشفت عن ظهور طور ثانوي إضافي من أكسيد الكوبالت. أظهرت الخصائص البصرية اختلافات ملحوظة مرتبطة بتركيز الكوبالت. يزداد الامتصاص البصري بشكل متناسب مع ارتفاع محتوى الكوبالت، بينما على العكس من ذلك، تنخفض فجوة الطاقة مع زيادة محتوى الكوبلت. تسلط هذه النتائج الضوء بشكل واضح على التوليف الذي يمكن التحكم فيه لهياكل ZnO النانوية الشبيهة بالجذور عن طريق الانحلال الحراري بالرش، والتي يتم تعديلها بواسطة التشويب بالكوبالت.

الكلمات المفتاحية: هندسة البنية النانوية، أكسيد فلز الأغشية الرقيقة، أكسيد الزنك المشوب بالكوبالت.

1. Introduction

In the realm of nanomaterials and thin film technology, the modification and manipulation of material properties at the nanoscale level have opened up unprecedented opportunities for enhancing functionality and performance across various applications [1]. Among these materials, zinc oxide (ZnO) thin films have garnered considerable attention due to their exceptional optical, electronic, and catalytic properties [2]. In recent years, researchers have been exploring novel approaches to engineer ZnO thin film nanostructures to unlock their full potential for advanced applications. One promising avenue involves the introduction of a specific dopant [3], or compose with different materials [4], coupled with the utilization of modification of deposition parameters such as rate of deposition through the simple technique of spray pyrolysis [5]. This combination offers a unique route to tailor the structural, optical, and electronic properties of ZnO thin films, thereby paving the way for the development of high-performance devices and systems [6].

The introduction of foreign atoms, into the lattice of a material can induce profound changes in its properties by altering its electronic structure, crystalline arrangement, and reactivity. Cobalt, a transition metal, has demonstrated intriguing dopant characteristics due to its unique electronic configuration and magnetic properties [7]. Incorporating cobalt dopants into ZnO thin films introduces an exciting avenue for enhancing their electronic conductivity, catalytic activity [8], and magnetic behaviour [9], making them well-suited for applications such as in optoelectronics [10].

Zinc Oxide exhibits diverse nanostructures that offer a wide range of unique properties and applications due to their exceptional characteristics. Some prominent nanostructure types of ZnO include Nanoparticles [11], Nanowires [12], Nanorods [13], Nanotubes [14], Nanobelts, and Nanoflowers [15], etc. Researchers continue to explore novel methods to fabricate and engineer these nanostructures to tailor their properties for specific applications [16].

Spray pyrolysis, on the other hand, represents a versatile deposition technique that allows for precise control over the growth process and resulting film morphology [17]. By employing low deposition rates during spray pyrolysis, it becomes possible to dictate the growth dynamics of ZnO thin films and induce the formation of distinctive nanostructures [18]. Of particular interest are root-like structures, which exhibit complex branching patterns that extend the surface area and alter the light-matter interaction, thereby affecting the optical and electronic properties of the films [19].

This paper aims to investigate into the intriguing interplay between cobalt doping, and low deposition rates using spray pyrolysis, and the resulting nanostructured ZnO thin films. Also, we investigate the effect of varying cobalt dopant concentrations on the optical and structural characteristics, as well as the energy bandgap of the ZnO films.

2. Materials and Method

Zinc acetate dihydrate (Zn $(CH_3COO)_2 \cdot$٢H_2O) of 99.99 % purity and cobalt acetate tetrahydrate $Co(CH_3CO_2)_2 \cdot$٤ H_2O of ≥98.0% purity from Sigma-Aldrich Co. were used with no further purification. 0.1M of the aqueous solution, at different Co^{+3}/Zn^{+2} ratios of (0, 0.1, 0.2, and 0.3), were prepared using a magnetic stirrer for 30 min. The Co-doped ZnO thin films were prepared by spray the precursors solution on corning glass at a fixed substrate temperature of 400 °C using an atomizer fixed at 30 cm vertically above the substrates. The solution is sprayed using a compressed air of 5 bar pressure at a low spray rate of 0.5 ml/min. The deposited samples were examined by X-ray diffraction (Shimadzu XRD 6000), SEM (JSM-7600F by JEOL Ltd), and UV-visible absorbance Metertech spectrophotometer (Model A).

3. Results and discussions

Figure 1 depicts X-ray diffraction (XRD) patterns illustrating the impact of Co^{+3}/Zn^{+2} ratios on pure and Co-doped ZnO thin films. These films were fabricated on Corning glass substrates using the spray pyrolysis technique. The resulting films exhibited polycrystalline nature characterized by a hexagonal wurtzite crystal structure. The observed XRD peaks corresponding to ZnO's crystalline planes, namely (100), (002), (101), (102), and (110), were in agreement with the JCPDS standard card (96-901-1663). Notably, the (101) plane displayed a preferred orientation. An increase in the Co content led to a reduction in crystallinity. Concurrently, a novel phase emerged corresponding to cubic cobalt oxide (Co_2O_3), as per the JCPDS standard card (96-900-5898). The preferential orientation for this cobalt structure occurred along the (220) plane. The appearance of a distinct phase at higher doping ratios resulted from the excessive introduction of Co beyond its capacity to be incorporated into the host lattice. The widening of peaks was observed with escalating doping ratios, indicating an augmentation in crystallite size as calculated using Sherrer's formula. Additionally, slight shifts in diffraction peaks suggested the presence of lattice strain due to the increasing dopant concentration. Information regarding peak positions, full width at half maximum (FWMH), inter-planar distances calculated using Bragg's law (equation 1) [20], and crystallite sizes determined through Sherrer's formula (equation 2) [21] can be found in Table 1. Figure 2 illustrates the growth in average crystallite size as a function of substrate temperature.

$$n\,\lambda = 2\,d_{hkl}\,\sin\theta \qquad \text{.................. (1)}$$

$$D = \frac{0.9\,\lambda}{FWHM\,.\cos(\theta)} \qquad \text{................. (2)}$$

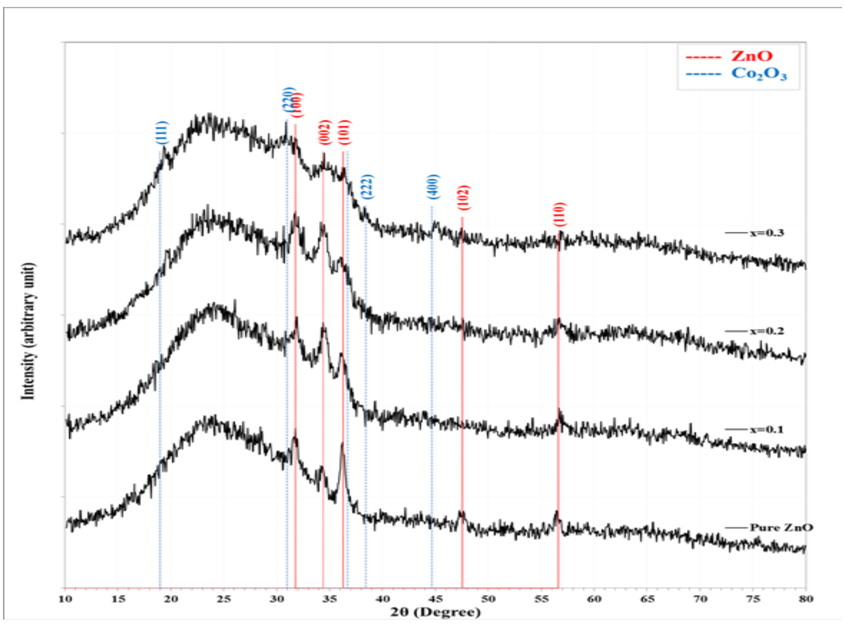

Fig. 1. X-ray diffraction for the as-deposited ZnO and Co-doped ZnO thin films at different ratios.

Table 1: XRD peaks parameters for the as-deposited ZnO and Co-doped ZnO thin films at different ratios.

x	2θ (Deg.)	FWHM (Deg.)	d_{hkl} Exp.(Å)	C.S (nm)	hkl	d_{hkl} Std.(Å)	Phase	ε
0	31.7532	0.6321	2.8158	13.1	(100)	2.8137	Hex. ZnO	0.0097
	34.2814	0.5794	2.6137	14.4	(002)	2.6035	Hex. ZnO	0.0082
	36.1776	0.5794	2.4809	14.4	(101)	2.4754	Hex. ZnO	0.0077
	47.5019	0.8427	1.9125	10.3	(102)	2.6035	Hex. ZnO	0.0084
	56.5087	0.8427	1.6272	10.7	(110)	2.6035	Hex. ZnO	0.0068
0.1	31.9112	1.1061	2.8022	7.5	(100)	2.8137	Hex. ZnO	0.0169
	34.5448	0.8954	2.5943	9.3	(002)	2.6035	Hex. ZnO	0.0126
	36.0722	0.6847	2.4879	12.2	(101)	2.4754	Hex. ZnO	0.0092
	56.6667	1.0007	1.6230	9.0	(110)	2.6035	Hex. ZnO	0.0081
0.2	19.6388	0.5268	4.5167	15.3	(111)	2.6035	Cubic. Co_2O_3	0.0133
	31.7005	0.8954	2.8203	9.2	(100)	2.8137	Hex. ZnO	0.0138
	34.4394	0.8954	2.6020	9.3	(002)	2.6035	Hex. ZnO	0.0126
	36.1249	0.9481	2.4844	8.8	(101)	2.4754	Hex. ZnO	0.0127
	56.6140	1.1061	1.6244	8.2	(110)	2.6035	Hex. ZnO	0.0090
0.3	19.2701	0.6321	4.6023	12.8	(111)	2.6035	Cubic. Co_2O_3	0.0162
	31.0500	0.4300	2.8779	19.2	(220)	2.4754	Cubic. Co_2O_3	0.0068
	31.7005	0.7374	2.8203	11.2	(100)	2.8137	Hex. ZnO	0.0113
	34.3868	0.8427	2.6059	9.9	(002)	2.6035	Hex. ZnO	0.0119
	36.2302	0.8428	2.4774	9.9	(101)	2.6035	Hex. ZnO	0.0112
	38.4110	0.3267	2.3416	25.8	(222)	2.6035	Cubic. Co_2O_3	0.0041
	45.1843	0.8954	2.0051	9.6	(400)	2.6035	Cubic. Co_2O_3	0.0094
	56.9300	0.7374	1.6162	12.3	(110)	2.6035	Hex. ZnO	0.0059

Lattice constants for hexagonal structure of ZnO (a and c) were determined according to the relation [22]:

$$\frac{1}{d_{hkl}^2} = \frac{4}{3}\frac{h^2+hk+k^2}{a^2} + \frac{l^2}{c^2} \quad \text{........ (3)}$$

The incorporation of cobalt ions with an unusual ionic radius into the host lattice resulted in structural deformation. This deformation led to a reduction in the c/a ratio compared to the ideal structure's close-packed ratio of 1.886. The maximum value of the "c" constant, in comparison with the lesser value of "a," was observed at x=0.1, indicating a particular composition. These structural deformations were induced by the incorporation of Co^{+3} ions with slightly greater ion radii than Zn^{+2} ion. Different manners of variations were observed for ZnO structure with different dopants [23,24].

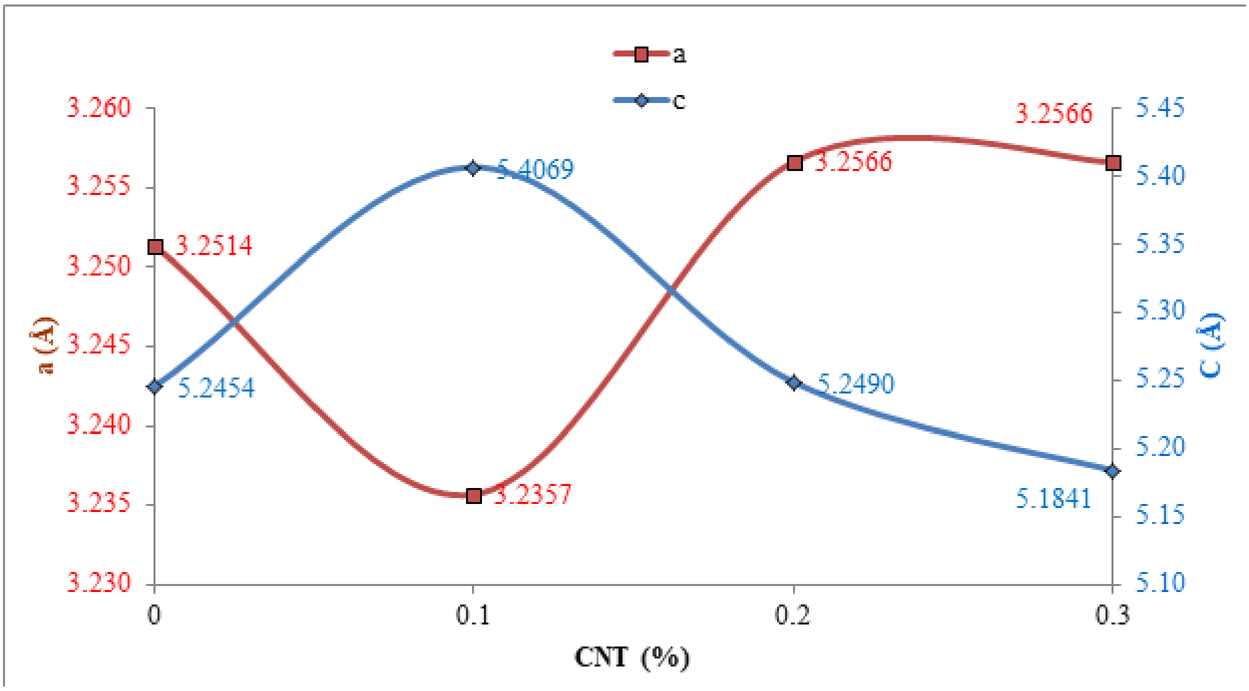

Fig. 2. Variation of lattice constants for ZnO with the Co ratio.

Figure 3 illustrates scanning electron microscope (SEM) images showcasing the morphological characteristics of as-deposited thin films of pure ZnO and Co-doped ZnO on glass substrates by spray pyrolysis.

Distinctive structural features manifest as novel root-like formations on the surface of the samples, resembling branched and intricate winding roots. With an increase in the concentration of Cobalt dopants within the samples, there is an observable increase in the diameters of these root structures. Specifically, for the pristine ZnO sample, the root diameter measures at 143 nm. However, upon introducing Cobalt dopants at ratios of x = 0.1, 0.2, and 0.3, the root diameters expand significantly, measuring 350 nm, 550 nm, and 570 nm, respectively.

In the case of the highest Co content sample (x = 0.3), the roots exhibit a merged configuration with the surface, lacking well-defined edges. Importantly, it is noteworthy to mention that prior research [25] has demonstrated diverse nanostructural configurations for ZnO thin films, achieved through various fabrication techniques. Notably, our observed root-like configuration aligns with the nanostructures reported in a previous study [26].

The ability to precisely control both the shape and size of these nanostructures holds remarkable implications for targeted applications of the prepared samples. This level of control opens avenues for leveraging these materials in specific applications such as insert specific applications where the tailored nanostructures could be beneficial.

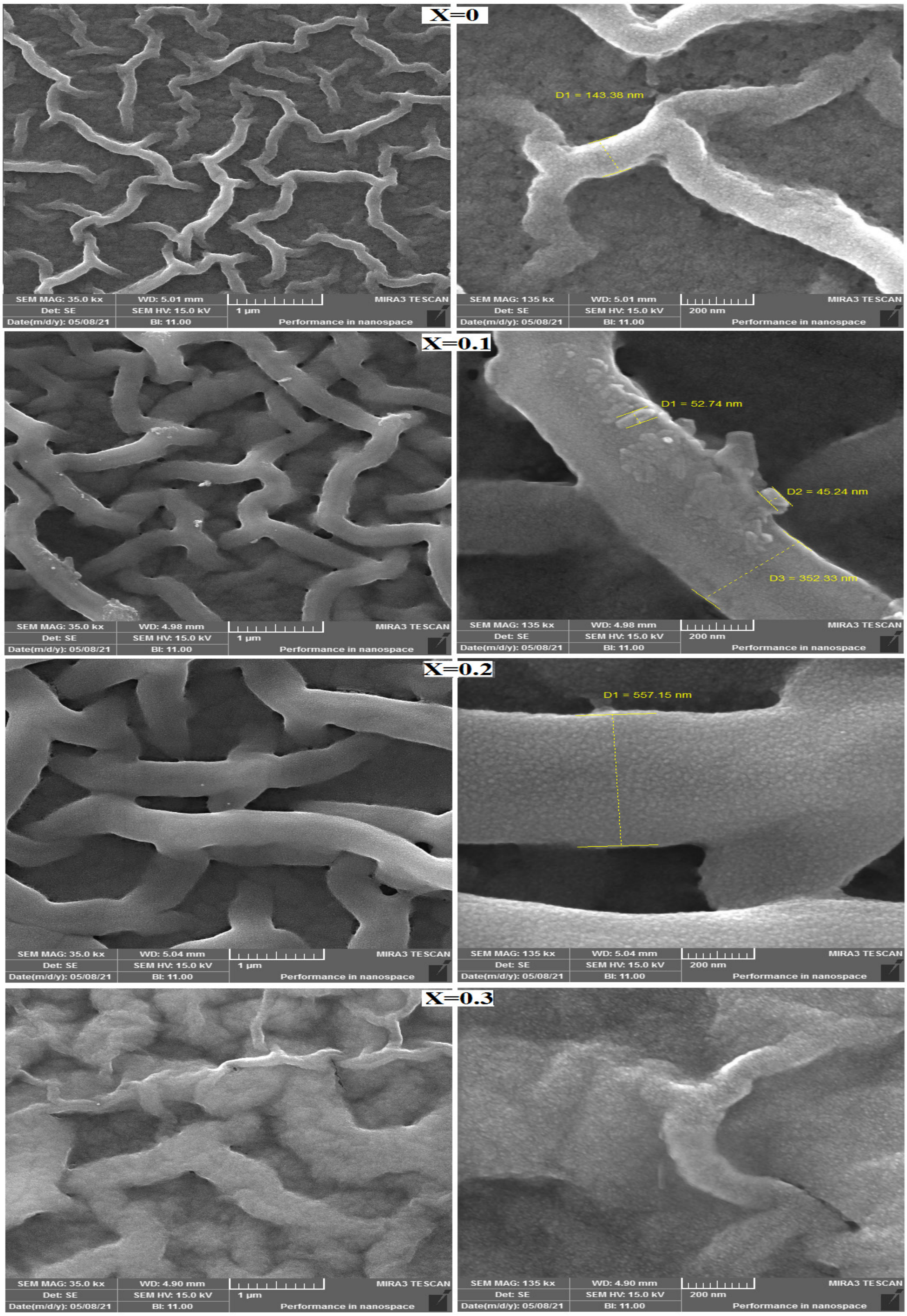

Fig. 3. SEM images for the as-deposited ZnO and Co-doped ZnO thin films at different ratios.

Figure 4 illustrates the optical absorbance spectra of Cobalt-doped ZnO films prepared by spraying on glass floors at different Co/Zn atomic ratios. It can be seen that the absorbance decreases with increasing wavelength for all samples prepared because only photons with sufficient energy greater than the energy gap can interact with the material forming electron pairs at the absorption edge. The absorption spectral characterization is affected by the material components. It can be seen that the absorbance increased with the Co content. It can be seen that the absorption edge is not sharp for all samples, which depends on the degree of crystallinity due to the presence of local states near the valence and conduction bands (tail states) [27].

The impurities at as active centers cause more light scattering and play an important role in determining the transparency of the material [28].

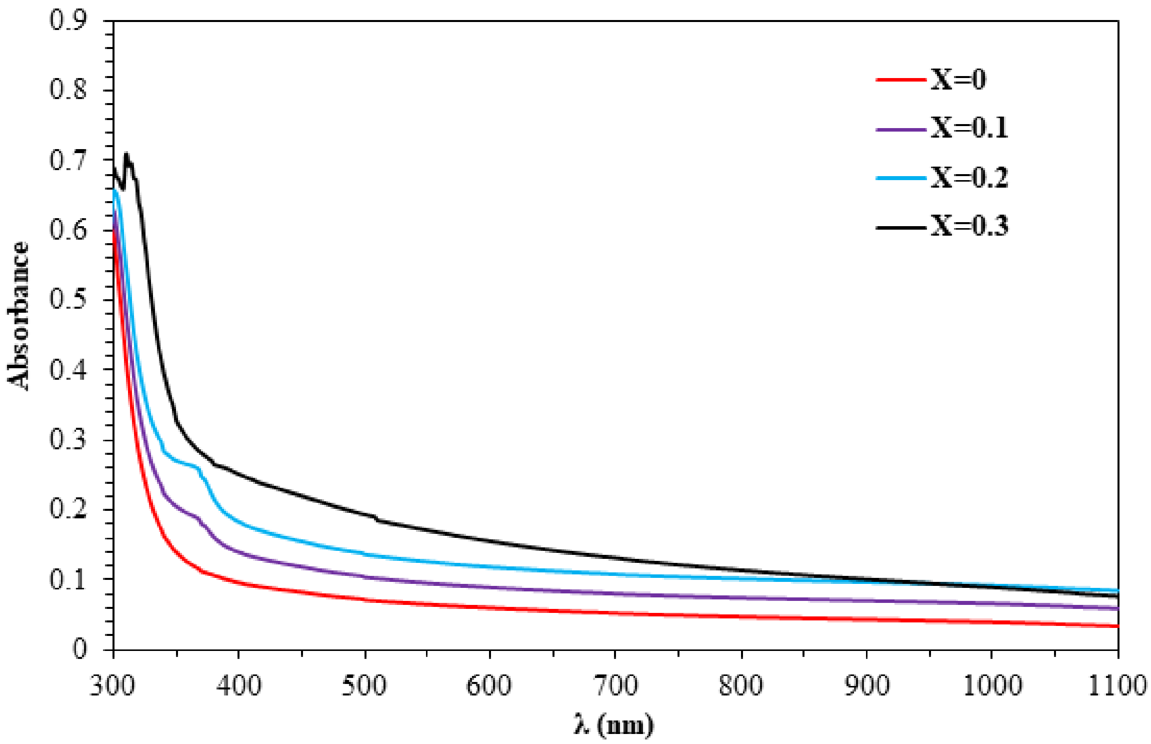

Fig. 4. Optical absorbance for the as-deposited ZnO and Co-doped ZnO thin films at different ratios.

The optical band gap (E_g^{opt}) of the Cobalt-doped ZnO films prepared by spraying on glass substrates at different Co/Zn atomic ratios was calculated using Tauc's equation for direct allowed transition [29].

$$\alpha h\nu = Constant\ (h\nu - E_g^{opt})^{1/2} \quad ......(4)$$

By plotting the relationship between $(\alpha h\nu)^2$ vs photon energy $h\nu$ as shown in Fig. 5. It was observed that the optical energy gap decreases from 3.9 eV to 3.6 eV when increasing the Cobalt content from 0 to 0.4 may due to creating new energy levels within the energy bandgap. The observed changes in the optical properties of the ZnO indicate that the Co^{3+} successfully replaced Zn^{2+} inside the hexagonal ZnO wurtzite structure [30].

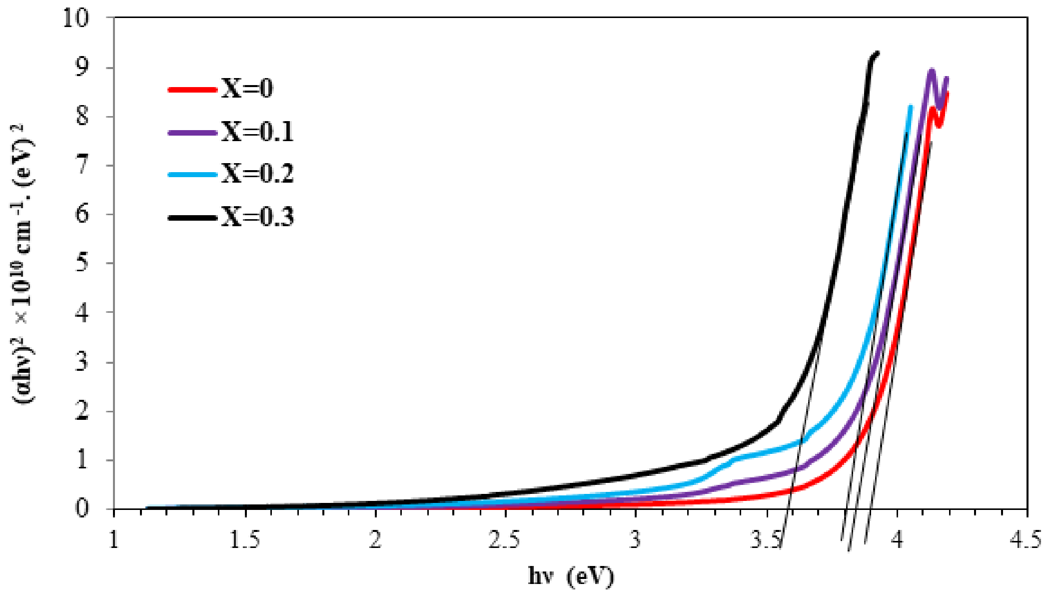

Fig. 5. Tauc relation for the as-deposited ZnO and Co-doped ZnO thin films at different ratios.

4. Conclusions

Utilizing the spray pyrolysis technique, root-like nanostructures of ZnO were effectively synthesized. This process involved the deposition of a metal acetate solution onto a heated platform maintained at 400 °C, while modulating the deposition rate. Concurrently, incremental incorporation of Cobalt dopants within the ZnO matrix was employed, resulting in a corresponding gradual enlargement of the root branches' diameter. Insight into the structural integrity was gained through X-ray diffraction (XRD) analysis. This investigation unveiled the successful incorporation of Cobalt dopants up to a concentration of x=0.2, wherein a coherent solubility was observed. However, at higher Co ratios, surpassing 0.3, the emergence of cobalt oxide as a distinct phase became discernible. A profound influence on the optical characteristics was observed in correlation with the variation in Co concentration. Specifically, the optical absorbance exhibited an ascending trend concurrent with the augmentation of Co content. This phenomenon. Conversely, the energy bandgap of the materials exhibited a diminishing trend in response to escalating Co content. These findings collectively underline the controllable fabrication of root-like ZnO nanostructures through the spray pyrolysis technique, modulated by Cobalt dopants. This work underscores the prospect of tailoring material characteristics for specific applications through controlled doping and highlights the consequential effects on structural and optical properties.

References

1. G. H. Jeong, S. P. Sasikala, T. Yun, G. Y. Lee, W. J. Lee, and S. O. Kim, Nanoscale Assembly of 2D Materials for Energy and Environmental Applications, Advanced Materials **32**(35), 1907006 (2020).
2. S. Madhavanunni Rekha, H. Vadakke Neelamana, and S. V. Bhat, Recent Advances in Solution-Processed Zinc Oxide Thin Films for Ultraviolet Photodetectors, ACS Applied Electronic Materials **5**(8), 4051–4066 (2023).
3. E. Benrezgua, B. Deghfel, A. Zoukel, W. J. Basirun, R. Amari, A. Boukhari, M. K. Yaakob, S. Kheawhom, and A. A. Mohamad, Synthesis and properties of copper doped zinc oxide thin films by sol-gel, spin coating and dipping: A characterization review, Journal of Molecular Structure **1267**, 133639 (2022).
4. M. A. Kadhim, M. O. Salman, and A. A. Ramadhan, "Effect of adding graphene on structural, surface morphology and optical properties of ZnO:SnO2 composite," in *The 9th International Conference on Applied Science and Technology*

(ICAST 2021) (2022), p. 030007.

5. P. Abraham, S. Shaji, D. A. Avellaneda, J. A. Aguilar-Martínez, and B. Krishnan, (002) oriented ZnO and ZnO:S thin films by direct ultrasonic spray pyrolysis: A comparative analysis of structure, morphology and physical properties, Materials Today Communications **35**, 105909 (2023).
6. E. Kärber, T. Raadik, T. Dedova, J. Krustok, A. Mere, V. Mikli, and M. Krunks, Photoluminescence of spray pyrolysis deposited ZnO nanorods, Nanoscale Research Letters **6**(1), 359 (2011).
7. J. Kazmi, P. C. Ooi, B. T. Goh, M. K. Lee, M. F. M. Razip Wee, S. Shafura A Karim, S. R. Ali Raza, and M. A. Mohamed, Bi-doping improves the magnetic properties of zinc oxide nanowires, RSC Advances **10**(39), 23297–23311 (2020).
8. N. R. Khalid, A. Hammad, M. B. Tahir, M. Rafique, T. Iqbal, G. Nabi, and M. K. Hussain, Enhanced photocatalytic activity of Al and Fe co-doped ZnO nanorods for methylene blue degradation, Ceramics International **45**(17), 21430–21435 (2019).
9. P. R. Chithira and T. Theresa John, Correlation among oxygen vacancy and doping concentration in controlling the properties of cobalt doped ZnO nanoparticles, Journal of Magnetism and Magnetic Materials **496**, 165928 (2020).
10. S. Shahzad, S. Javed, and M. Usman, A Review on Synthesis and Optoelectronic Applications of Nanostructured ZnO, Frontiers in Materials **8**, (2021).
11. S. Mohan, S. Sudarsan, E. Parthiban, S. Guhanathan, and S. V. S. Prasad, Synthesis and characterization of binding interaction of ZnO nanoparticles with organic compounds, Materials Today: Proceedings (2023).
12. A. Feng, C. Lin, H. Zhou, W. Jin, Y. Hu, D. Li, and Q. Li, Catalytic transformation of 4-nitrophenol into 4-aminophenol over ZnO nanowire array-decorated Cu nanoparticles, Green Chemical Engineering (2023).
13. B. Poornaprakash, U. Chalapathi, K. Subramanyam, S. V. P. Vattikuti, and S.-H. Park, Wurtzite phase Co-doped ZnO nanorods: Morphological, structural, optical, magnetic, and enhanced photocatalytic characteristics, Ceramics International

46(3), 2931–2939 (2020).

14. C. Zhao, L. Li, Y. Zhu, and L. Zhang, Performance study of photocatalytic hydrogen production from ZnO double-walled nanotubes based on density functional theory, Computational and Theoretical Chemistry **1225**, 114179 (2023).
15. Q. Ma, F. Cui, J. Zhang, and T. Cui, Built-in electric field boosted ionic transport kinetics in the heterostructured ZnCo2O4/ZnO nanobelts for high-performance supercapacitor, Journal of Colloid and Interface Science **629**, 649–659 (2023).
16. M. A. Deshmukh, H. N. Thorat, M. D. Shirsat, and A. Ramanavicius, “Engineered nanostructures: an introduction,” in *Engineered Nanostructures for Therapeutics and Biomedical Applications* (Elsevier, 2023), pp. 1–43.
17. N. Winkler, A. Wibowo, B. Kubicek, W. Kautek, G. Ligorio, E. List-Kratochvil, and T. Dimopoulos, Rapid Processing of In-Doped ZnO by Spray Pyrolysis from Environment-Friendly Precursor Solutions, Coatings **9**(4), 245 (2019).
18. J. Cho, S. Hwang, D.-H. Ko, and S. Chung, Transparent ZnO Thin-Film Deposition by Spray Pyrolysis for High-Performance Metal-Oxide Field-Effect Transistors, Materials **12**(20), 3423 (2019).
19. M. Srivathsa, P. Kumar, and B. V. Rajendra, Ultraviolet photoconductivity and photoluminescence properties of spray pyrolyzed ZnO nanostructure: Effect of deposition temperature, Optical Materials **131**, 112726 (2022).
20. W. H. Bragg and W. L. Bragg, *X Rays and Crystal Structure* (G. Bell and Sons, LTD., 1918).
21. A. S. H. Hameed, C. Karthikeyan, A. P. Ahamed, N. Thajuddin, N. S. Alharbi, S. A. Alharbi, and G. Ravi, In vitro antibacterial activity of ZnO and Nd doped ZnO nanoparticles against ESBL producing Escherichia coli and Klebsiella pneumoniae, Scientific Reports **6**(April), 1–11 (2016).
22. M. A. Basyooni, M. Shaban, and A. M. El Sayed, Enhanced Gas Sensing Properties of Spin-coated Na-doped ZnO Nanostructured Films, Nature Publishing Group **7**(August 2016), 1–12 (2017).

23. S. Saleem, M. H. Jameel, N. Akhtar, N. Nazir, A. Ali, A. Zaman, A. Rehman, S. Butt, F. Sultana, M. Mushtaq, J. H. Zeng, M. Amami, and K. Althubeiti, Modification in structural, optical, morphological, and electrical properties of zinc oxide (ZnO) nanoparticles (NPs) by metal (Ni, Co) dopants for electronic device applications, Arabian Journal of Chemistry **15**(1), 103518 (2022).

24. U. ur Rehman, K. ul Sahar, K. Mahmood, M. Kanwal, A. Ashfaq, M. F. Iqbal, H. Wang, N. Al-Zaqri, E. Hussain, and A. A. Khan, Effect of Ni and Mn dopant on thermoelectric power generation performance of ZnO nanostructures synthesized via hydrothermal method, Materials Chemistry and Physics **304**, 127907 (2023).

25. R. Kumar and Kamakshi, "Synthesis routes of ZnO nanocrystallites," in *Nanostructured Zinc Oxide* (Elsevier, 2021), pp. 23–56.

26. P. Ramesh, A. Rajendran, and M. Meenakshisundaram, Green Syntheis of Zinc Oxide Nanoparticles Using Flower Extract Cassia Auriculata, Journal of NanoScience and NanoTechnology **2**(1), 41–45 (2014).

27. G. Mei-Zhen, Z. .Feng, L. Jing, and S. .Hui-Na, Effect of annealing conditions on properties of sol-gel derived Al-doped ZnO thin films, J. Chinese Phys. Lett **26**, 1–7 (2019).

28. L. K. Gaur, P. Gairola, S. P. Gairola, M. C. Mathpal, P. Kumar, S. Kumar, D. Kushavah, V. Agrahari, F. F. H. Aragon, M. A. G. Soler, and H. C. Swart, Cobalt doping induced shape transformation and its effect on luminescence in zinc oxide rod-like nanostructures, Journal of Alloys and Compounds **868**, 159189 (2021).

29. S. Q. Haza'a and H. R. Shaker, Effect of Thickness on Structural, Optical and Sensing Properties of SnS Thin Films Prepared by Ultrasonic Nebulizer Method, International Journal of Thin Films Science and Technology **7**(3), 105–112 (2018).

30. G. A. Alharshan, A. M. Aboraia, M. A. M. Uosif, I. M. Sharaf, E. R. Shaaban, M. Saad, H. ALMohiy, and M. M. Elsenety, Optical Band Gap Tuning, DFT Understandings, and Photocatalysis Performance of ZnO Nanoparticle-Doped Fe Compounds, Materials **16**(7), 2676 (2023).